ELSEVIER

Journal of Nuclear Materials 270 (1999) 334–341

journal of nuclear materials

Thermal stability and brazing characteristics of $Zr_{0.7-x}M_xBe_{0.3}$ (M = Ti or Nb) ternary amorphous filler metals

Young-Soo Han [a], Choon-Ho Park [b], Kuk-Jin Jang [a], Cha-Hurn Bae [c], Chang-Burm Choi [b], Jai-Young Lee [a,*]

[a] *Department of Materials Science and Engineering, Korea Advanced Institute of Science and Technology, Kusong-Dong 373-1, Yusung-Gu, Taejon, South Korea*

[b] *Fuel Technology Center, Korea Nuclear Fuel, 150 Duckjin-Dong, Yusung-Gu, Taejon, South Korea*

[c] *PuKyong National University, 559-1 Daeyeon, 3-Dong, Nam-Gu, Pusan, South Korea*

Received 25 September 1998; accepted 5 December 1998

Abstract

The effects of Ti or Nb substitution on the thermal stability and brazing characteristics of $Zr_{0.7-x}M_xBe_{0.3}$ (M = Ti or Nb) ternary amorphous alloys were investigated in order to improve properties of Zr–Be binary amorphous alloy as a new filler metal for joining zirconium alloy. The $Zr_{0.7-x}M_xBe_{0.3}$ (M = Ti or Nb; $0 \leqslant x \leqslant 0.1$) ternary amorphous alloys were produced by melt-spinning method. In the selected compositional range, the thermal stability of $Zr_{0.7-x}Ti_xBe_{0.3}$ and $Zr_{0.7-x}Nb_xBe_{0.3}$ amorphous alloys are improved by the substitution of titanium or niobium for zirconium. As the Ti and Nb content increases, the crystallization temperatures increase from 610°C to 717°C and 610°C to 678°C, respectively. These amorphous alloys were put into practical use in joining bearing pads on zircaloy cladding sheath. Using Zr–Ti–Be amorphous alloys as filler metals, smooth interface and spherical primary particles (proeutectic phase) appear in the brazed layer, which is the similar microstructure of using $Zr_{0.7}Be_{0.3}$ binary amorphous alloys. In the case of Zr–Nb–Be amorphous alloys, Ni-precipitated Zr phase that may cause some degradation in ductility and corrosion-resistance is formed at both sides of the brazed layer.

PACS: 61.43.Er; 65.90.+i

1. Introduction

In manufacturing of CANDU and CANFLEX fuel bundles, various components (spacer pads, bearing pads, buttons etc.) are joined by brazing process on the surface of cladding sheath of zirconium alloy [1]. Physically vapor-deposited (PVD) metallic beryllium has currently been used as a brazing filler metal [2]. In this case, the chemical toxicity of beryllium vapor requires very complicated PVD process for physical protection [3]. There are also several shortcomings such as reduction of sheath wall and the difficulty of microstructural control due to the nature of diffusion brazing [4,5].

In previous paper we reported that Zr–Be binary amorphous alloys with hypo-eutectic composition were better filler metal and could overcome a lot of disadvantages caused by the use of conventional PVD Be metal [6]. Using Zr–Be amorphous alloys as filler metals, the reduction in thickness of cladding sheath wall can be prevented. Especially, in the case of using the hypo-eutectic compositional amorphous alloys, such as $Zr_{0.65}Be_{0.35}$ and $Zr_{0.7}Be_{0.3}$, smooth interface and spherical primary α-Zr particles appear in the brazed layer. It is more favorable morphology in brazed interfaces than PVD Be metal and other Zr–Be amorphous alloys with hyper-eutectic composition in the view of the corrosion-resistance [6]. However, the thermal stability of Zr–Be

* Corresponding author. Tel.: +82-42 869 3313; fax: +82-42 869 8910; e-mail: jailee@sorak.kaist.ac.kr

0022-3115/99/$ – see front matter
PII: S0022-3115(99)00007-0

binary amorphous alloys is not good for the practical blazing process. The temperatures and activation energies for crystallization are too low [7,8]. Therefore, for the application of Zr–Be binary amorphous alloy as a brazing filler metal, its thermal stability must be improved.

In this work, in order to improve the thermal stability of Zr–Be binary amorphous alloy, Ti or Nb has been partially substituted for Zr in $Zr_{0.7}Be_{0.3}$ binary amorphous alloy that could be the best filler metal for joining zirconium alloys. The amorphous formability and the thermal stability of $Zr_{0.7-x}M_xBe_{0.3}$ (M = Ti or Nb) ternary amorphous alloys are investigated and the microstructure of the joints brazed by using Zr–M–Be (M = Ti or Nb) amorphous ribbons are also characterized.

2. Experimental

The $Zr_{0.7-x}M_xBe_{0.3}$ (M = Ti or Nb) alloys, where x was ranged from 0 to 0.1, were prepared from materials with 99.9 w/o purity by means of arc-melting under an inert atmosphere of argon and were remelted three times for homogeneity. These alloys have hypo-eutectic compositions in Zr–Be binary alloy system. Amorphous ribbons were prepared by the melt-spinning method [9,10] in low pressure of argon. The alloys were heated to about 1000°C (above the corresponding liquidus temperature) in a quartz tube by high frequency induction heating. And then they were injected by argon pressure of 0.7 atm onto the copper wheel that was rotating at tangential speed of 45 m/s in the Ar atmosphere to prevent oxidation of ribbons. The thickness and width of ribbons were about 30 μm and 1.5 mm, respectively.

The amorphization of these ribbons with various compositions of Ti and Nb was examined by X-ray diffractometer (Rigaku D/MAX-IIIC) with Cu-Kα radiation. In order to investigate the crystallization behavior and thermal stability of the amorphous ribbons, thermal analysis was conducted with differential scanning calorimeter (Perkin–Elmer DSC-7). The amorphous ribbons were heated from 30°C to 650°C with the different heating rates of 10, 20, 30 and 50°C/min under Ar gas flow to estimate the crystallization temperatures and activation energy though Kissinger plot [11].

On the other hand, after the amorphous ribbons as filler metals were located between bearing pads (2.5 × 30 × 1.5 mm) and a Zircaloy-4 cladding sheath (a tube of 0.4 mm thick and 13 mm diameter), the pads were temporarily and mechanically joined on the sheath by press. And then brazing was carried out at 10^{-5} Torr and 1050°C for 20 s. Two series of $Zr_{0.7-x}Ti_xBe_{0.3}$ and $Zr_{0.7-x}Nb_xBe_{0.3}$ amorphous ribbons ($x = 0.01$, 0.03, 0.05, 0.07 and 0.1) were used as filler metals. The cross-section of the brazed layers between Zircaloy-4 cladding sheath tube and bearing pads was observed by scanning electron microscopy (SEM). And the thickness and mor-

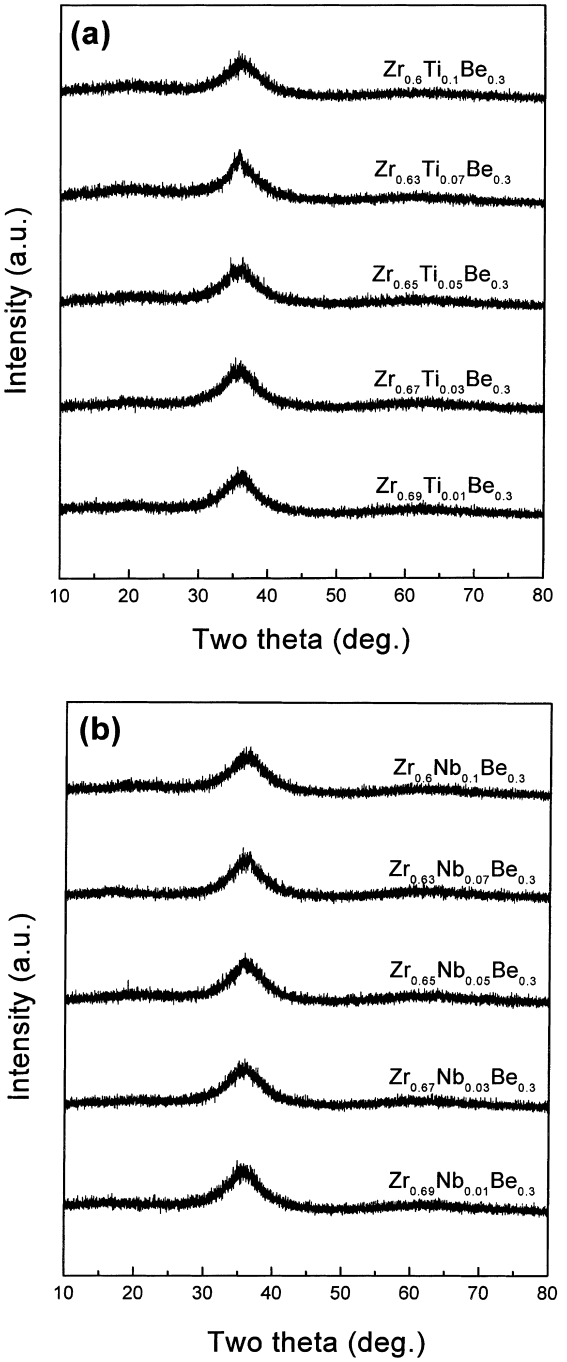

Fig. 1. X-ray diffraction patterns of (a) $Zr_{0.7-x}Ti_xBe_{0.3}$ and (b) $Zr_{0.7-x}Nb_xBe_{0.3}$ ($x = 0.01$, 0.03, 0.05, 0.07, 0.1) ribbons prepared by melt spinning method.

phology of the brazed layer were evaluated with respect to the content of Ti and Nb substituted for Zr in the $Zr_{0.7-x}M_xBe_{0.3}$ (M = Ti or Nb) filler metals.

3. Results and discussion

3.1. The formation and thermal stability of $Zr_{0.7-x}M_xBe_{0.3}$ (M = Ti or Nb; $0 \leqslant x \leqslant 0.1$) amorphous alloys

The X-ray diffraction (XRD) patterns of the $Zr_{0.7-x}Ti_xBe_{0.3}$ and $Zr_{0.7-x}Nb_xBe_{0.3}$ ($x = 0.01$, 0.03, 0.05, 0.07, 0.1) ribbons made by melt-spinning method are shown in Fig. 1(a) and (b), respectively. There are no distinguishable peaks in these patterns throughout the experimental compositions except only a broad peak centered in vicinity of 36° which is observed from all XRD patterns. From these results, it can be seen that the $Zr_{0.7-x}M_xBe_{0.3}$ (M = Ti or Nb; $0 \leqslant x \leqslant 0.1$) ribbons prepared by melt-spinning are amorphous alloys [7].

The DSC results obtained from the ribbons having different amount of Ti or Nb are shown in Fig. 2 (a) and (b), respectively. In the both cases of $Zr_{0.7-x}Ti_xBe_{0.3}$ and $Zr_{0.7-x}Nb_xBe_{0.3}$ ($0 \leqslant x \leqslant 0.1$) ternary amorphous alloys, two exothermic peaks are observed, which is similar to $Zr_{0.7}Be_{0.3}$ binary amorphous alloy. In our previous work [6], it has been proved that the crystallization of $Zr_{0.7}Be_{0.3}$ amorphous alloys proceeds through two steps. In the first step the Zr–Be amorphous alloy transforms to the α-Zr phase and another amorphous phase at the relatively low temperature. In the second step the $ZrBe_2$ phase is formed from remaining amorphous phase at relatively high temperature. It is found that this crystallization behavior also can be applied to the $Zr_{0.7-x}Ti_xBe_{0.3}$ and $Zr_{0.7-x}Nb_xBe_{0.3}$ ternary system in the compositional range of $0 \leqslant x \leqslant 0.07$ as shown in Fig. 2.

Fig. 3(a) and (b) show the variations of crystallization temperatures (T_x) of the first peak and second peak in DSC curves as a function of Ti and Nb content. The crystallization temperatures of both ternary amorphous alloys increase gradually as the content of titanium or niobium increases. Especially, the increasing rate of crystallization temperature in the $Zr_{0.7-x}Ti_xBe_{0.3}$ amorphous alloys is larger than that in $Zr_{0.7-x}Nb_xBe_{0.3}$ amorphous alloys. That is, as the Ti and Nb atomic ratios increase from 0 to 0.1, the crystallization temperatures of $Zr_{0.7-x}M_xBe_{0.3}$ (M = Ti or Nb) ternary amorphous alloys increase from 610°C to 717°C and 610°C to 678°C, respectively.

The activation energy (ΔE_x) of a crystallization reaction can be determined by Kissinger equation [11],

$$\mathrm{d}\ \ln(\phi/T_\mathrm{p}^2)/\mathrm{d}\ (1/T_\mathrm{p}) = -\Delta E_x/R,$$

where ϕ is heating rate, T_p is peak temperature in DSC curve and R is gas constant. The Kissinger plots of the

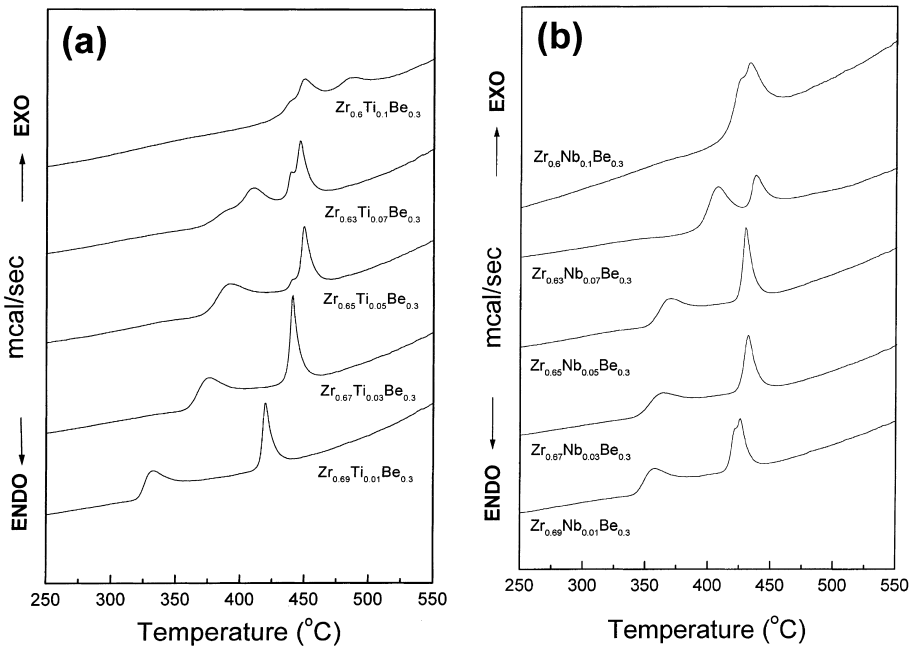

Fig. 2. DSC curves of (a) $Zr_{0.7-x}Ti_xBe_{0.3}$ and (b) $Zr_{0.7-x}Nb_xBe_{0.3}$ ($x = 0.01$, 0.03, 0.05, 0.07, 0.1) ternary amorphous alloys at 20°C/min heating rate.

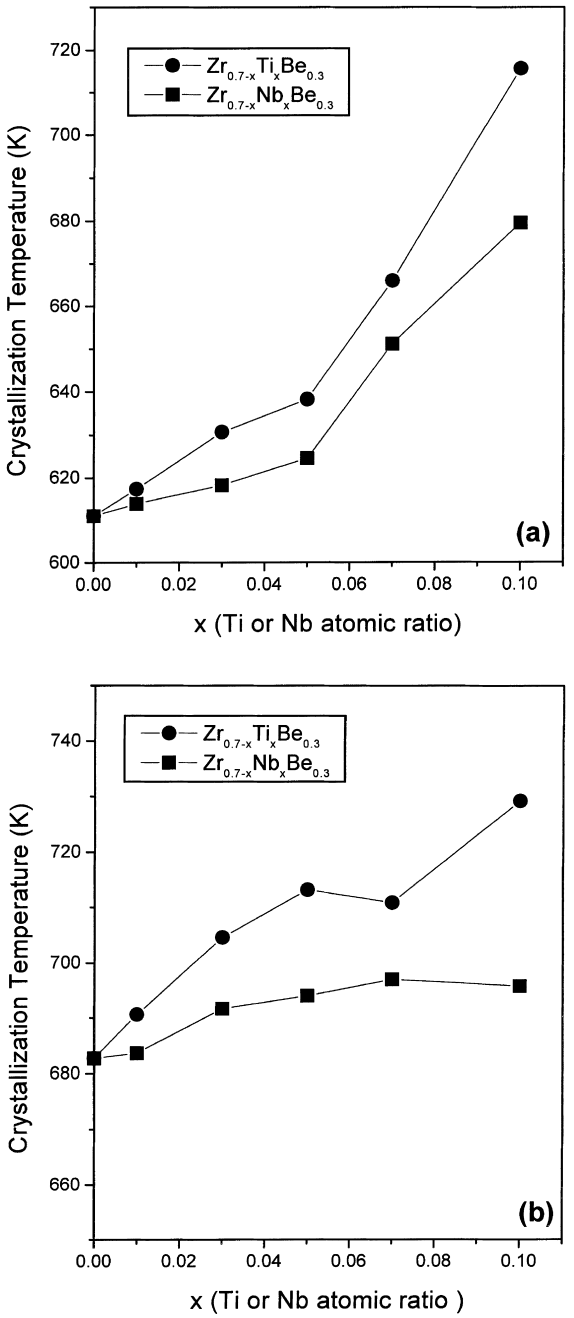

Fig. 3. Crystallization temperatures for (a) the first peak reaction and (b) the second peak reaction of Zr–X–Be (X = Nb or Ti) ternary amorphous alloys in DSC curves.

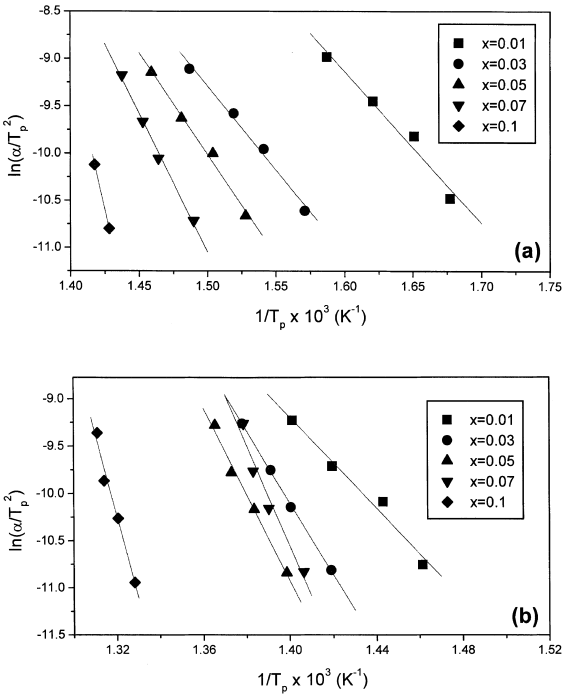

Fig. 4. Kissinger plots for (a) the first peak reaction and (b) the second peak reaction of $Zr_{0.7-x}Ti_xBe_{0.3}$ ($x = 0.01$, 0.03, 0.05, 0.07, 0.1) alloys in DSC curves.

first and second exothermic reactions are shown in Figs. 4 and 5. The activation energies calculated from the slope of these plots are replotted as a function of Ti or Nb atomic ratio in Fig. 6. In $Zr_{0.7-x}Ti_xBe_{0.3}$ ($0 \leqslant x \leqslant 0.1$) ternary amorphous alloys, the activation energy of the first reaction varies from 41.25 to 57.62 kcal/mol and that of the second one varies from 68.24 to 106.1 kcal/mol. In the case of $Zr_{0.7-x}Nb_xBe_{0.3}$ ternary amorphous alloys, the activation energy of the first reaction increases from 41.25 to 47.5 kcal/mol with the increase of Nb content but that of the second one is not changed significantly in the compositional range of $0 \leqslant x \leqslant 0.1$.

From the above results shown in Figs. 3 and 6, it is found that the thermal stability of Zr–Be binary amorphous alloy can be improved by the partial substitution of titanium and niobium for zirconium. Especially, the substitution of Ti is more effective than that of Nb in the $Zr_{0.7-x}Ti_xBe_{0.3}$ and $Zr_{0.7-x}Nb_xBe_{0.3}$ ($0 \leqslant x \leqslant 0.1$) ternary amorphous alloys. These results may be explained from the atomic size effect. Walter [12] explained the enhancement of thermal stability of $Fe_{82-x}M_xB_{18}$ (M = Ni, Co, Cr, V, Pt, Mo, Au, Nb, Si and Dy) in terms of the difference of atomic radius. In Zr–M–Be (M = Ti, Nb) ternary system the atomic radii of zirconium, titanium and niobium are 0.216, 0.200 and 0.208 nm, respectively. The partial substitution of titanium and niobium for zirconium can cause the lattice distortion, which may prohibit the diffusion and ordering of Zr and Be atoms for the crystallization of the Zr–M–Be (M = Ti, Nb) ternary amorphous alloys. As the atomic radius of Ti is

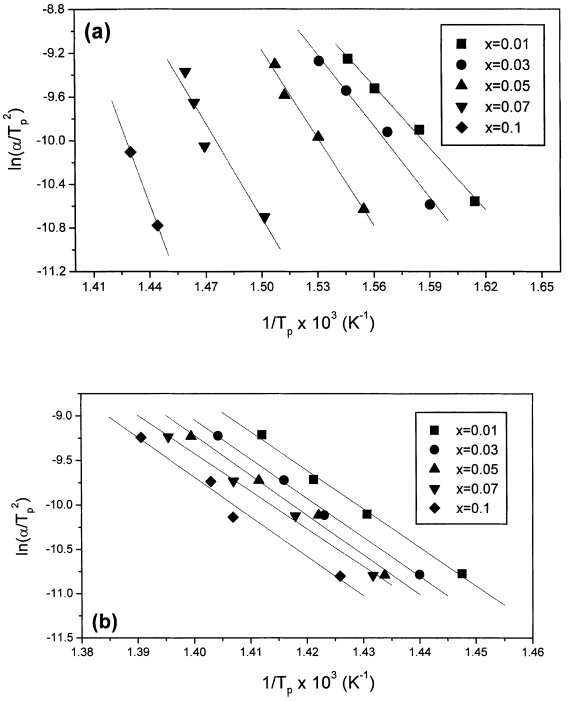

Fig. 5. Kissinger plots for (a) the first peak reaction and (b) the second peak reaction of $Zr_{0.7-x}Nb_xBe_{0.3}$ ($x = 0.01$, 0.03, 0.05, 0.07, 0.1) alloys in DSC curves.

smaller than that of Nb, it is considered that the partial substitution of Ti for Zr is more effective than that of Nb to improve the thermal stability of Zr–Be binary amorphous alloy.

3.2. Microstructure of the brazements

Bearing pads were brazed on the surface of cladding sheath with $Zr_{0.7-x}M_xBe_{0.3}$ (M = Ti or Nb: $x = 0.01$, 0.03, 0.05, 0.07, 0.1) ternary amorphous ribbons of 30 μm thick as filler metals at 1050°C. The microstructures of the brazed layers of two systems were analyzed with SEM as shown in Figs. 7 and 8, respectively. In the case of $Zr_{0.7-x}Ti_xBe_{0.3}$ ternary amorphous alloys the morphology of the brazed layer is not changed noticeably in the selected composition range. Only the width of the brazed layer increases slightly with the content of titanium. On the other hand, in the case of the $Zr_{0.7-x}Nb_xBe_{0.3}$ ternary amorphous ribbons there is no increase in the width of the brazed layer compared with that of the layer (ca. 23 μm thick) brazed with $Zr_{0.7}Be_{0.3}$ binary amorphous filler metal. But the morphology of the brazed layer is changed drastically. New region is found at both sides of the brazed layer and broadened gradually with the increase of Nb content. Fig. 9(a) shows the EDS

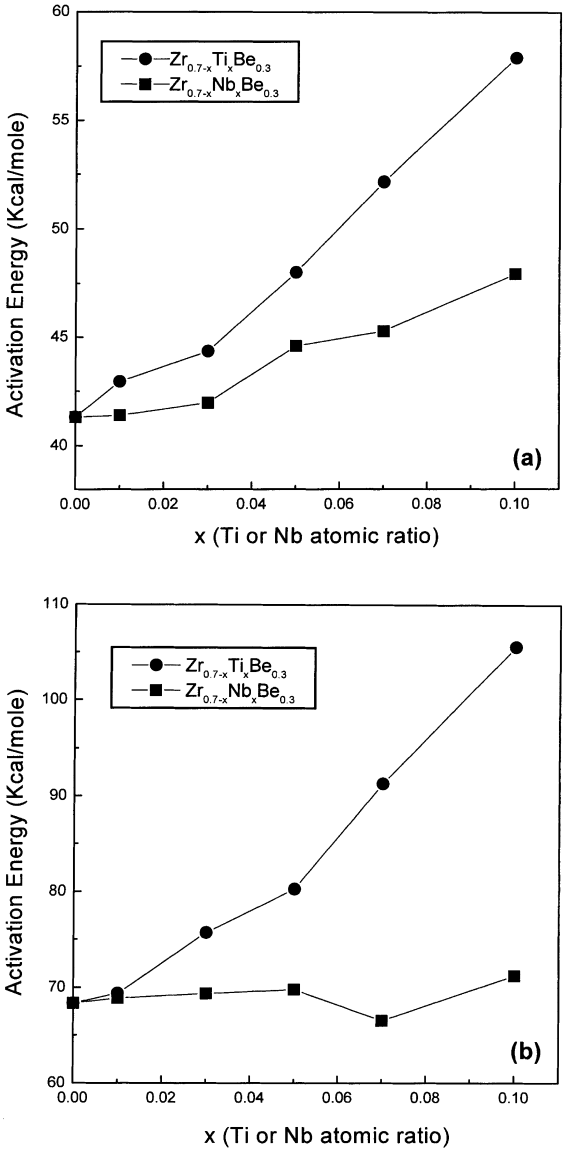

Fig. 6. Activation energies for (a) the first peak reaction and (b) the second peak reaction of Zr–X–Be (X = Nb or Ti) ternary amorphous alloys in DSC curves.

spectrum of the new region (***B*** part in Fig. 8(e)). Zr–K_α and Nb–K_α peaks appear at 15.747 and 16.584 KeV, respectively. From this EDS spectrum it is found that Nb content is 6.08 at.% in the region, which is extremely high in comparison with the solubility of Nb in Zr matrix below ~620°C as shown in Fig. 9(b) [13]. Therefore it is considered that this region may be composed of Zr matrix phase and the Nb-rich second phase whose formation is due to the 'miscibility gap' between zirconium and niobium as shown in Fig. 9(b). Zr–Nb binary system exhibits complete liquid and solid

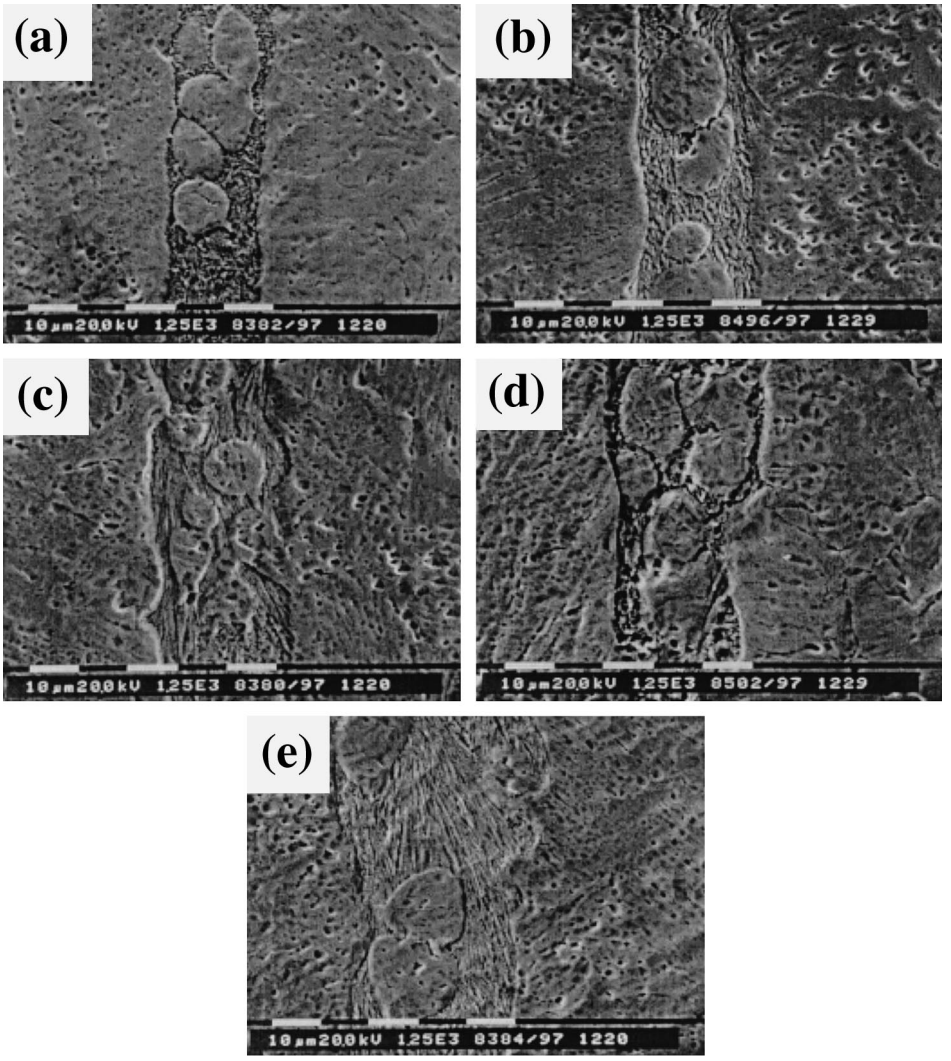

Fig. 7. SEM photographs of the interfaces brazed with (a) $Zr_{0.69}Ti_{0.01}Be_{0.3}$, (b) $Zr_{0.67}Ti_{0.03}Be_{0.3}$, (c) $Zr_{0.65}Ti_{0.05}Be_{0.3}$, (d) $Zr_{0.63}Ti_{0.07}Be_{0.3}$, (e) $Zr_{0.6}Ti_{0.1}Be_{0.3}$ amorphous ribbons as filler metals.

solubility above 988°C. However it has miscibility gap below 988°C. In the case of the $Zr_{0.7-x}Nb_xBe_{0.3}$ ($0 \leqslant x \leqslant 0.1$) alloy, during and after brazing Nb is soluble completely in liquid and solid Zr matrix above ca. 860°C. But below the temperature of 860°C, Nb atoms supersaturate and precipitate in Zr matrix because of miscibility gap between Zr and Nb. Therefore 'Nb-precipitated Zr phase' is formed at the both sides of blazed layer.

From the above microstructural evolution of the brazed layers with the change of composition in the $Zr_{0.7-x}M_xBe_{0.3}$ (M = Ti or Nb; $0 \leqslant x \leqslant 0.1$) ternary amorphous filler materials, it is found that both ternary amorphous alloys are suitable for brazing of zirconium alloys in the view of preventing the reduction in thickness of cladding sheath wall like $Zr_{0.7}Be_{0.3}$ binary amorphous filler metal [6]. However, it has been well known that two-phase microstructure such as Nb-precipitated Zr phase appeared in Zr–Nb–Be ternary system are brittle and have low corrosion resistance [14]. So it is believed that $Zr_{0.7-x}Ti_xBe_{0.3}$ ternary amorphous alloys are better than $Zr_{0.7-x}Nb_xBe_{0.3}$ ones as filler metals from the viewpoint of corrosion resistance.

4. Conclusions

$Zr_{0.7-x}M_xBe_{0.3}$ (M = Ti or Nb) ternary amorphous alloys in the compositional range of $0 \leqslant x \leqslant 0.1$ were

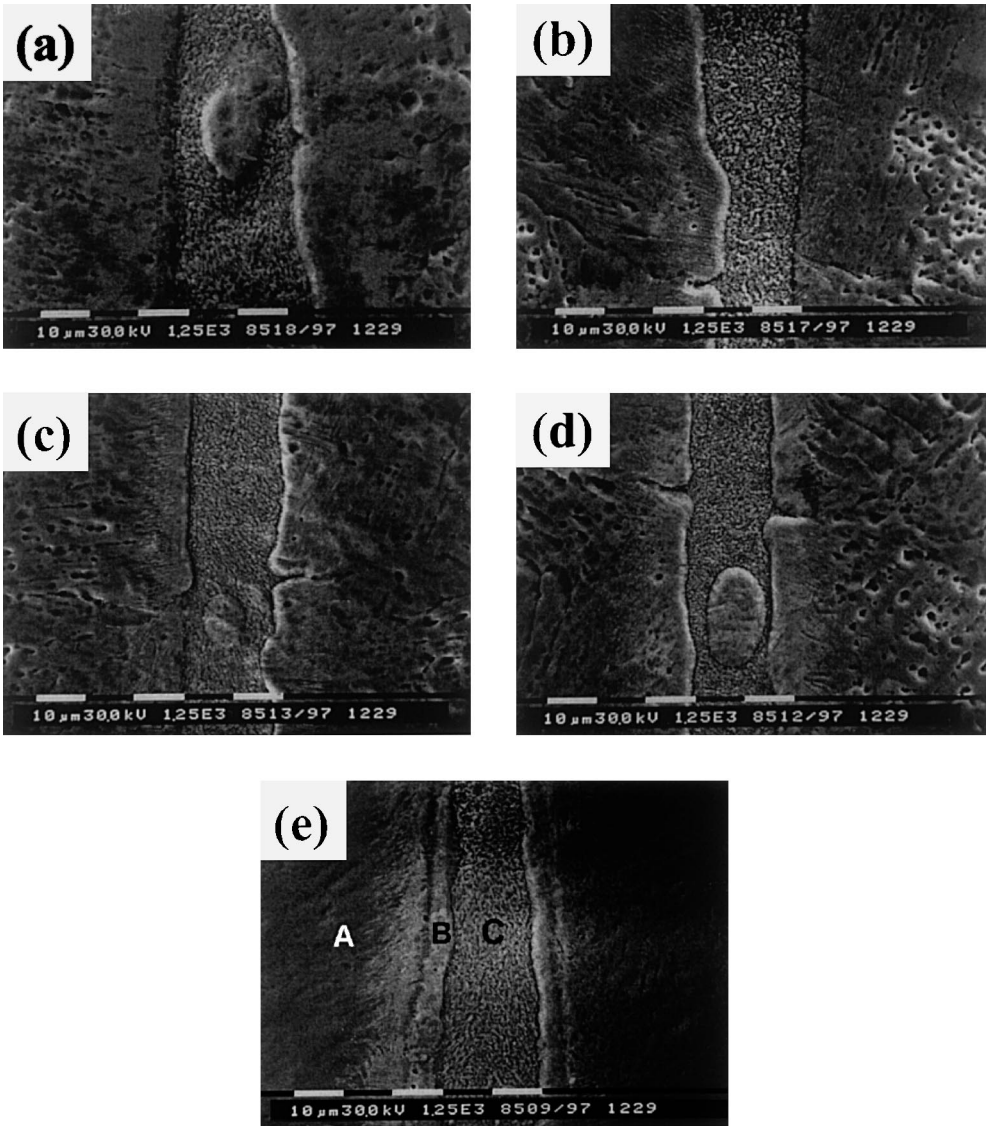

Fig. 8. SEM photographs of the interfaces brazed with (a) $Zr_{0.69}Nb_{0.01}Be_{0.3}$, (b) $Zr_{0.67}Nb_{0.03}Be_{0.3}$, (c) $Zr_{0.65}Nb_{0.05}Be_{0.3}$, (d) $Zr_{0.63}Nb_{0.07}Be_{0.3}$, (e) $Zr_{0.6}Nb_{0.1}Be_{0.3}$ amorphous ribbons as filler metals.

produced by melt-spinning method. The crystallization behaviors of the $Zr_{0.7-x}M_xBe_{0.3}$ (M = Ti or Nb) ternary amorphous alloys were similar to those of $Zr_{0.7}Be_{0.3}$ binary amorphous alloys, which proceeded through two exothermic reactions.

The $Zr_{0.7-x}M_xBe_{0.3}$ (M = Ti or Nb) ternary amorphous alloys had better thermal stability than $Zr_{0.7}Be_{0.3}$ binary amorphous alloys. As the content of Ti and Nb substituted for Zr increased from 0% to 10%, the crystallization temperatures of $Zr_{0.7-x}M_xBe_{0.3}$ (M = Ti or Nb) ternary amorphous alloys increased from 610°C to 717°C and 610°C to 678°C. And the activation energy increased from 41.25 to 57.62 kcal/mol and 41.25 to 47.5 kcal/mol, respectively.

In the case of $Zr_{0.7-x}Ti_xBe_{0.3}$ ternary amorphous alloys as filler metals, the morphology and thickness of the brazed layers were not changed in comparison with those of the layers brazed with $Zr_{0.7}Be_{0.3}$ binary amorphous alloys. Using the $Zr_{0.7-x}Nb_xBe_{0.3}$ ternary amorphous alloys, the formation of Nb-precipitated Zr phase was observed at both sides of the brazed layer.

It is suggested that $Zr_{0.7-x}Ti_xBe_{0.3}$ ternary amorphous alloys are better filler metals for joining of Zr alloy than

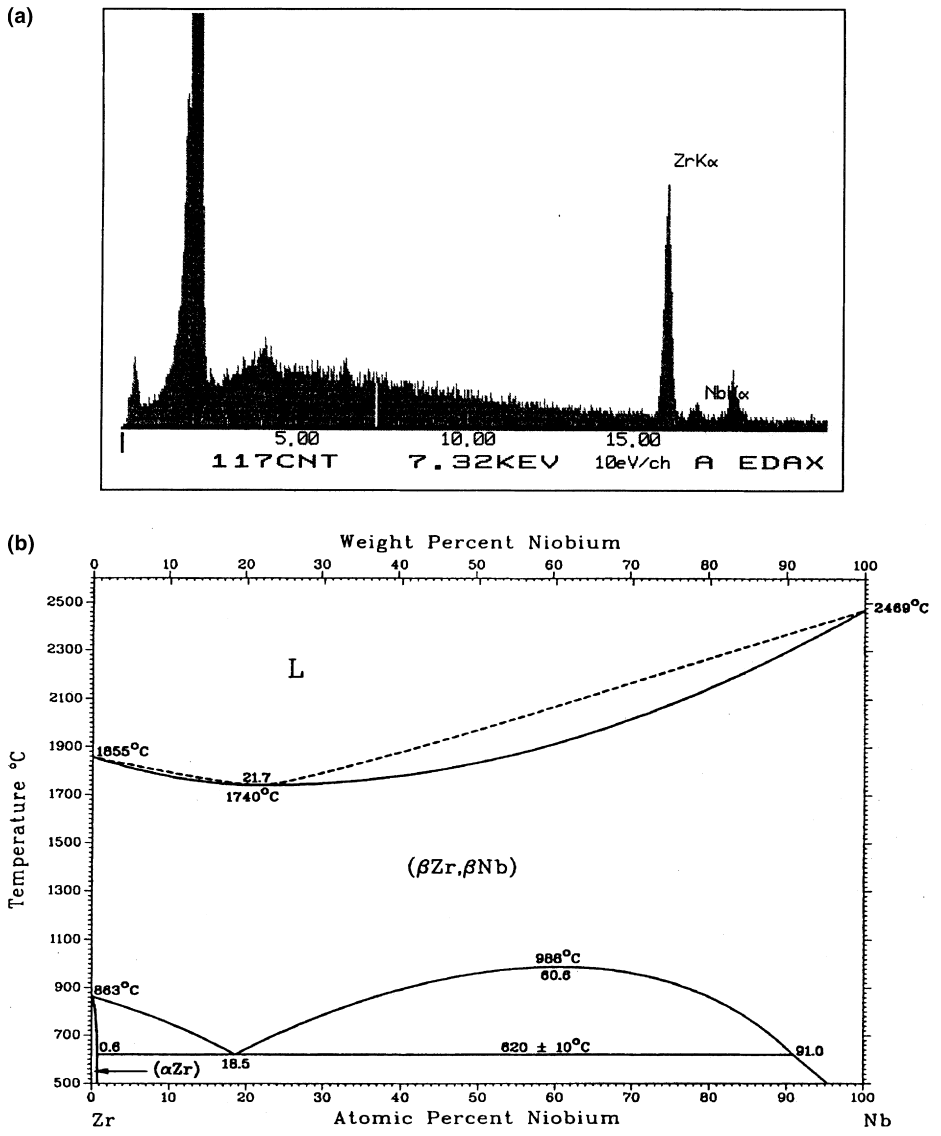

Fig. 9. (a) EDS spectra of ***B*** part in Fig. 8(e) and (b) Zr–Nb binary phase diagram [13].

$Zr_{0.7-x}Nb_xBe_{0.3}$ ternary amorphous alloys in the viewpoint of thermal stability and corrosion resistance.

References

[1] R.D. Page, Atomic Energy of Canada Ltd. Report, AECL-5609, Canadian Power Reactor Fuel, 1976.
[2] G. Mcgregor, Process for brazing Zirconium alloy elements, Canadian Patent No. 883578, 1971.
[3] P.J. Apencer, O.V. Goldbeck, Beryllium Physicochemical Properties of its compounds and alloys, Atomic Energy Review, 1978.
[4] J. Amato, F. Baudrocco, M. Ravizza, Welding J. 51 (7) (1972) 341.
[5] N. Bredz, H. Schwarzwart, Welding J. 37 (8) (1959) 305.
[6] C.H. Park, Y.S. Han, J.Y. Lee, J. Nucl. Mater. 254 (1998) 34–41.
[7] L.E. Tanner, R. Ray, Acta Metall 27 (1979) 1727.
[8] G.F. Syrykh, A.P. Zhernov, M.N. Kholopkin, A.V. Suetin, J. Non-Cryst. Solids 181 (1995) 244.
[9] P. Duwez, Trans. Am. Soc. Met. 60 (1967) 607.
[10] R.W. Cahn, P. Hassen, Physical Metallurgy, Elsevier Science, Amsterdam, 1983.
[11] H.E. Kissinger, Anal. Chem. 29 (1957) 1702.
[12] J.L. Walter, Mater. Sci. Eng. 50 (1981) 137.
[13] T.B. Massalski, Binary Alloy Phase Diagrams, 2nd ed., Alloy Phase Diagram International Commission.
[14] M.G. Fontana, Corrosion engineering, 3rd ed., McGraw-Hill, Singapore, 1988.